Influence of electric arc furnace dust and lime kiln waste in Portland cement hydration

Influência do pó de forno elétrico a arco e lama de carbonato de calico na hidratação do cimento Portland

Josué Claudio Metz
Elenize Ferreira Maciel
Marilise Garbin
Regina Célia Espinosa Modolo
Carlos Alberto Mendes Moraes
Lucas Bonan Gomes
Feliciane Andrade Brehm

Abstract

Studies have indicated that the use of electric arc furnace dust (EAFD) results in a delay in the hydration time of Portland cement. Calcium-rich waste such as lime kiln waste (LKW) is one of the techniques used to offset this delay as it accounts for the lack of this element in calcium silicate hydrate (C-S-H) production in the mixture. The objective of this study was to evaluate the influence of electric arc furnace dust (EAFD) and lime kiln waste (LKW) in the hydration process of Portland cement pastes and their influence in setting time and hydration heat. The methodology used required several steps: physiochemical and micro-structural characterization of waste samples; definition and production cement pastes with different levels of waste substitution and a reference paste and evaluation of the cement pastes with respect to setting time and hydration heat. Results showed that the substitution of 1% EAFD with or without LKW presented similar hydration heats as the reference paste. This indicated that EAFD+LKW substitution would not affect substantially the hydration reactions of cement and could allow waste recycling in construction materials.

Keywords: Electric arc furnace dust. Lime kiln waste. Portland cement hydration. Portland cement pastes.

[1]Josué Claudio Metz
[1]Universidade do Vale do Rio dos Sinos
São Leopoldo – RS – Brasil

[2]Elenize Ferreira Maciel
[2]Universidade Federal do Rio Grande do Sul
Porto Alegre – RS – Brasil

[3]Marilise Garbin
[3]Universidade do Vale do Rio dos Sinos
São Leopoldo – RS – Brasil

[4]Regina Célia Espinosa Modolo
[4]Universidade do Vale do Rio dos Sinos
São Leopoldo – RS – Brasil

[5]Carlos Alberto Mendes Moraes
[5]Universidade do Vale do Rio dos Sinos
São Leopoldo – RS – Brasil

[6]Lucas Bonan Gomes
[6]Universidade Federal do Rio Grande do Sul
Porto Alegre – RS – Brasil

[7]Feliciane Andrade Brehm
[7]Universidade do Vale do Rio dos Sinos
São Leopoldo – RS – Brasil

Recebido em 01/02/20
Aceito em 03/06/20

Resumo

Estudos realizados com o pó de forno elétrico a arco (PAE) indicam um retardo no tempo de hidratação do cimento Portland. A incorporação de resíduos ricos em cálcio, como a lama de carbonato de cálcio (LCC), é uma das formas de redução deste retardo, a fim de suprimir a deficiência deste elemento para a produção de C-S-H. Este estudo teve como objetivo avaliar a influência do uso do PAE, combinado ou não com o LCC no processo de hidratação de pastas de cimento em relação ao tempo de pega e calor de hidratação. A metodologia utilizada envolve a caracterização física, química e microestrutural das amostras de resíduos, a formulação e produção de pastas de cimento com diferentes teores de substituição de resíduose sem substituição (amostra de referência) e a avaliação das propriedades das pastas de cimento em relação ao tempo de pega e à evolução do calor de hidratação. Os resultados mostraram que a substituição de 1% de PAE combinado ou não com LCC apresentaram um calor de hidratação semelhante à amostra referência, sugerindo que nessa quantidade, a incorporação de PAE+LCC não afetaria significativamente as reações de hidratação do cimento, possibilitando a reciclagem destes resíduos em materiais de construção.

***Palavras-chave**: Pó de forno elétrico a arco. Lama de carbonato de cálcio. Hidratação do cimento Portland. Pasta de cimento Portland.*

Introduction

Steel production is an important economic activity that generates high levels of waste. In 2017, for each metric ton of raw steel produced in Brazil, 600 kg of waste and co-products were generated (INSTITUTO…, 2018). Electric arc furnace dust (EAFD) is a waste generated in the fusion of scrap steel as heavy metals are volatilized, oxidized, later solidified and captured in specialized exhaust system cleaning dust filters (KAVOURAS *et al.*, 2007; NIUBÓ *et al.*, 2009; CARRANZA *et al.*, 2016). This waste contains oxides from different metals such as Zn, Cd, Pb and Cr, which many countries recover through pyrolitic or hydrometallurgic processes (VARGAS; MASUERO; VILELA, 2004). The amount of EAFD generated for each metric ton of steel produced varies between 10 kg to 20 kg (STEGEMANN *et al.*, 2000; MENAD *et al.*, 2003). Around the world, it is estimated that 70% of EAFD is disposed in industrial landfills and 30% are processed for Zn recovery and other purposes (MASLEHUDDIN *et al.*, 2011). In Brazil, most EAFD are disposed in industrial landfills (INSTITUTO…, 2018).

Another important sector of Brazilian industry is paper and cellulose. In 2018, the Brazilian eucalyptus production averaged 36 m³/ha per year while the *pinus* production averaged 30 m³/ha. In the same time period, 52 million metric tons of related solid waste were produced, of which 70.9% originated from wood extraction and 29.1% originated from industrial activity (IBÁ, 2019). This waste includes dregs ($CaCO_3$ and Na_2CO_3), grits ($CaCO_3$ and CaO) and calcium carbonate lime kiln waste (LKW) which are of interest due to their potential applications in agriculture and construction (SIQUEIRA; HOLANDA, 2013; MODOLO *et al.*, 2010). Part of LKW is discarded in the Kraft process used in industry. Most LKW is repurposed as raw material for calcium replacement and only becomes true waste when the replacement process is interrupted, which can occur in the following situations:

(a) furnace maintenance;

(b) excess production; or

(c) high level of impurities in the LKW.

In these cases LKW is not used in recovery techniques and is disposed adequately (WOLFF, 2008; MODOLO *et al.*, 2014).

The final destination of industrial waste is a rising concern for waste-generating companies as environmental and legal requirements are becoming more restrictive. In many European countries, higher taxes on the use of industrial landfills are applied as an incentive to the use of more economically viable solutions. This combination offers an opportunity in the development of new sustainable practices regarding waste and co-products which can be used as raw materials for other distinct industrial activities (BURUBERRI; SEABRA; LABRINCHA, 2015; FISCHER; LEHENER; MCKINNON, 2011).

The construction sector is a field with great potential for the reuse of recycled waste from other industry sectors due to its sheer volume of activity. Construction demands large quantities of raw materials which contain both material and energetic production costs, especially in the case of steel and cement. Thus, in this sector, there is a demand for research and assessment on the reuse and recycling of industrial waste.

The use of EAFD in cement and concrete has already been studied. However, EAFD substitution has always been in limited quantities since the Zn content in EAFD tends to delay the initial setting time of cement, compromising its use as a construction material (AL-ZAID; AL-SUGAIR; AL-NEGHEIMISH, 1997; BREHM *et al.*, 2017; VARGAS; MASUERO; VILELA, 2006; MASLEHUDDIN *et al.*, 2011; CUBUKCUOGLU; OUKI, 2012; FARES *et al.*, 2016; ARNOLD; VARGAS; BIANCHINI, 2017). Despite this caveat, according to Al-Zaid, Al-Sugair and Al-Negheimish (1997), when added in quantities of less than 1 wt%, ZnO presence in EAFD does not significantly affect setting time. On the other hand, Massarweh *et al.* (2020) notes that EAFD can be purposely used in cement to delay hydration time in lieu of commercial retardants, thus prolonging the lifetime of concrete.

An alternative to curb the increase in the setting time is the further addition of Calcium-rich LKW in order to promote the production of calcium silicate hydrate (C-S-H) in the mixture (BREHM *et al.*, 2017). In face of these facts, the present study was conducted to evaluate the influence of electric arc furnace dust (EAFD) and lime kiln waste (LKW) in the hydration process of Portland cement pastes and their influence in setting time and hydration heat.

Methodology

The EAFD and LKW used in this studied are shown in Figure 1. Both wastes were obtained from local industries in the south of Brazil and samples were collected according to procedures listed in NBR 10007 (ABNT, 2004). The EAFD originated from steel produced in a semi-integrated mill which was captured in dust sleeves from the exhaust of the electric arc furnace (EAF) as part of the emission control. The LKW was generated in the causticizing step of the chemical recovery process of a cellulose and paper mill. These wastes were not further treated before being added to the cement pastes tested.

The cement used was a high early-strength type designated CPV-ARI which contains less than 10% carbonate filler addition according to NBR 16697 (ABNT, 2018c). Table 1 lists the physiochemical properties of CPV-ARI.

Figure 1 – **Sample of EAFD (A) and LKW (B)**

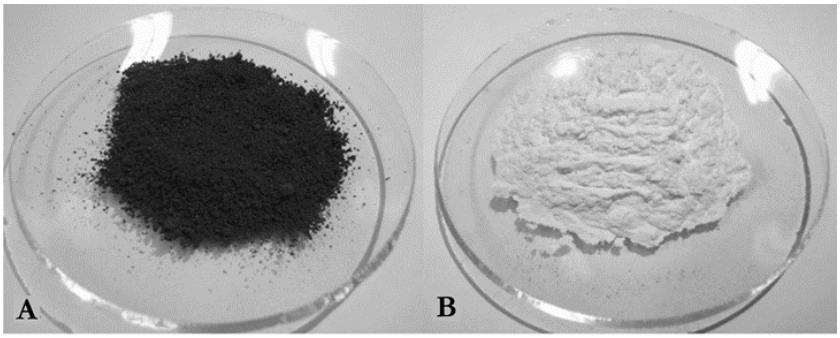

Table 1 – **Physical and chemical characteristics of cement CPV-ARI**

Physical tests	
Specific surface area – nitrogen adsorption (Brunauer-Emmett-Teller - BET) (m^2/g)*	1.20
Granulometry by laser diffraction (µm)**	D_{10}: 4.42
	D_{50}: 15.69
	D_{90}: 37.55
	D_{mean}: 17.53
Initial setting time (min)***	157
Final setting time (min)***	194
Fineness index 75 µm (wt%)***	0.46
Fineness index 45 µm (wt%)***	3.07
Normal consistency (%)***	28.4
Compressive strength 1 day (MPa)***	22.4
Compressive strength 3 days (MPa)***	37.7
Compressive strength 7 days (MPa)***	43
Compressive strength 28 days (MPa)***	51.2
Chemical tests (wt%)	
Aluminum oxide – Al_2O_3***	4.35
Silicon oxide – SiO_2***	18.91
Iron oxide – Fe_2O_3***	2.69
Calcium oxide – CaO***	60.59
Magnesium oxide – MgO***	4.74
Sulfur trioxide – SO_3***	2.86
Free calcium oxide – CaO free***	0.94
Loss on ignition***	2.89
Insoluble residue***	0.72
Alkaline equivalent***	0.62

Note: *analysis performed by the authors - Micromeritics, TriStar II Plus, Vacuum-degassed (200 °C) for 24 hours, 20 adsorption points were analyzed.**analysis performed by the authors - Particle Analyzer Microtrac - S3500, the wet analysis was conducted using isopropyl alcohol as solvent, one drop of surfactant at 50% and ultrasound time of approximately 10s. The refractive index used for samples was 1.52. D_{10}, D_{50}, D_{90} and D_{mean}: diameter of particles in 10%, 50%, 90% and mean of the retained fraction.***source: Companhia Cimento Itambé (2015).

The stages and methodologies applied in the study are shown in Table 2. Stage 1 determined the physiochemical and micro-structural characteristics of both wastes. Stage 2 formulated the cement pastes to be tested, starting from a baseline reference without substitution (REF) to varying levels of weight (wt%) substitution of pure EAFD and EAFD + LKW. Stage 3 analyzed the cement pastes formulated in Stage 2 with regards to setting time and hydration heat time evolution.

In **Stage 1**, samples were prepared with specific techniques for each step (Table 2).

In **Stage 2**, cement pastes were formulated with a stoichiometric quantity of LKW. The quantity of Ca needed was enough to form calcium zincate ($CaZn_2(OH)_6 2H_2O$) according to Equation 1:

$$2\ Zn(OH)_2 + 2OH^- + Ca^{2+} + 2\ H_2O \longrightarrow Ca\ Zn_2\ (OH)_6 \cdot 2H_2O \qquad \text{Eq. 1}$$

Table 2- **Stages and methodologies applied in the study**

	Objective	Test	Unit	Standard/Equipment/Parameters/Software
Stage 1	EAFD, LKW characteriz-ation	Granulometry by laser diffraction	µm	Samples were pre-dried in an oven at 105 ± 5 ºC for 4 hours. Equipment: Particle Analyzer Microtrac - S3500. The wet analysis was conducted using isopropyl alcohol (LKW) and water (EAFD) as solvent, one drop of surfactant at 25% (EAFD), 50% (LKW) and ultrasound time of approximately 10s. The refractive index used for samples was 1.52 (LKW) and 1.81 (EAFD).
		Moisture	%	Samples were dried in an oven at 105 ± 5 ºC. Equipment: Bel.
		Loss on ignition	%	Samples were pre-dried in an oven at 105 ± 5 ºC for 4 hours and subjected to temperatures between 525 ºC and 950 ºC in a laboratory kiln. Mass loss was measured in both processes. Standard: CEMP 120 (ABIFA, 2003).
		Specific mass	g/cm³	Samples were pre-dried in an oven at 105 ± 5 ºC for 4 hours. Equipment: Pycnometer Micromeritics, AccuPyc II 1340.
		Specific surface area - nitrogen adsorption (Brunauer-Emmett-Teller - BET)	(m²/g)	Samples were pre-dried in an oven at 105 ± 5 ºC for 4 hours. Equipment: Micromeritics, TriStar II Plus. Vacuum-degassed (350 ºC - EAFD and 200 ºC - LKW) for 24 hours. For each sample, 20 adsorption points were analyzed.
		Optical emission spectrometry by Inductively Coupled Plasma (ICP-OES) - Elementary Chemical Composition	%	Samples were broken down by microwave equipment following EPA Method 3015a (EPA, 2007) with either nitric acid (HNO_3) or a combination of nitric acid (HNO_3) and hydrochloric acid (HCl). Equipment: Microwave Titan MPS, Perkin Elmer
		X-ray Diffraction (XRD)	%	Samples were pre-dried in an oven at 105 ± 5 ºC for 4 hours and ground in an agate mortar and pestle to yield grains with a granulometry of less than 44 µm. Equipment: Diffractometer PANalytical, Empyrean, with fixed anode tube of Cu, operating at 45 kV and 40 mA. Ranges: 10º to 90º 2θ for LKW and 10º to 70º 2θ for EAFD, step 0.013º 2θ at 51.5s (detector in linear mode). Without monochromator and with fixed slots: divergent slot: 1/4°; incident anti-scatter crack: 1°; mask: 20 mm, diffracted anti-scatter crack: 17.8 mm, angular range collected by linear detector: 6.34°.
		Method of Rietveld	%	Software MAUD (Material Analysis Using Diffraction).
Sta-ge 2	Cement pastes' formulation	Normal consistency	%	Standard: NBR 16606 (ABNT, 2018a).
Stage 3	Evaluation of the properties of cement pastes	Setting time	Min	Standard: Vicat apparatus following NBR 16607 procedures (ABNT, 2018b).
		Evolution of semi-adiabatic temperature	ºC	Equipment: Chamber with semi-adiabatic thermal insulation.
		X-ray Diffraction (XRD)	%	Equipment: Diffractometer PANalytical, Empyrean, with fixed anode tube of Cu, operating at 45 kV and 40 mA. Ranges: 10º a 70º 2θ step.
		Rietveld Method	%	Software MAUD (Material Analysis Using Diffraction).

Based on the chemical composition data of Table 4, LKW levels to be added were determined as 0.11g of LKW with 51.66 wt% of Ca for each 1g of EAFD containing 24.16 wt% of Zn. The water/cement ratio (w/c) used in setting time and semi-adiabatic temperature tests were in accordance with NBR 16006 (ABNT, 2018a) to yield a cement paste of normal consistency. Cement pastes were prepared in cylindrical molds of 16 mm x 32 mm made from rigid, non-absorbing material and aged in a humidity-controlled chamber for 1 day, 4 days and 7 days. After demolding, cement pastes were immersed in isopropyl alcohol for 24h to stop hydration and kept in an oven at 60 ^{o}C until tested. Table 3 shows the different compositions of cement pastes tested.

In Stage 3, hydration heating was monitored in a semi-adiabatic, thermally-insulated chamber. Cement pastes were placed in aluminum cans (300 mL, 400 g ± 10 g) with K-type thermocouples inserted in their center and connected to a Pico Log data acquisition system. For each measurement, 6 pastes were monitored simultaneously. Pastes REF, 1EA, 1EA-LK, 10EA and 10EA-LK aged 1day, 4 days and 7 days were also subjected to Rietveld refinement to determine the phases formed for each time period.

Results and discussion

Physiochemical characterization of EAFD and LKW waste

Detailed chemical composition results for EAFD and LKW obtained from ICP - OES is shown in Table 4. EAFD was found to contain mostly Fe (31.30 wt%) and Zn (24.06 wt%) with a Ca quantity of 1.82 wt%. Results also showed the presence of Cd, Pb and Cr in mass fractions of 0.01%, 0.98% and 0.29%, respectively. EAFD moisture content was measured as 1.63% at 105 °C while total loss on ignition from both temperatures (550 ^{o}C and 950 ^{o}C) from a dry base was of 6.90 wt%. LKW was found to contain more than 50% mass fraction of Ca (51.66 wt%) followed by a small presence of Na (0.89 wt%). Other elements were present in mass fractions of less than 0.5 wt% such as Si (0.31 wt%), Mg (0.27 wt%) and Al (0.13 wt%). LKW is composed mainly from calcium carbonate ($CaCO_3$), small quantities of magnesium carbonate ($MgCO_3$) and other trace minerals (MODOLO *et al.*, 2014). LKW moisture content at 105 °C was of 2.85% while dry base loss on ignition at 550 ^{o}C and 950 ^{o}C were 12.65 wt% and 13.81 wt%, respectively, for a total of 24.46 wt%. This may be the result of Portlandite dehydroxylation ($Ca(OH)_2$) which occurs at temperatures between 450 ^{o}C and 550 ^{o}C and calcite ($CaCO_3$) decomposition which occurs at temperatures between 700 ^{o}C and 900 ^{o}C (ALARCON-RUIZ *et al.*, 2005).

The granulometric distributions shown in Figure 2 demonstrate considerable variations of mean particle sizes of EAFD, LKW and cement: 0.69 µm, 29.06 µm and 17.53 µm, respectively. The meanparticle size can affect cement in various ways: porosity, packing, hydration rate and water consumption (AIQIN; CHENGZHI; NINGSHENG, 1999; KNOP; PELED, 2016). In this case, since EAFD had a mean particle size smaller than cement while LKW presented the opposite, there was an increase in granulometric distribution that could positively affect packing and decrease porosity and water consumption.

Table 3 - **Composition of Portland cement pastes**

Paste	Cement (wt%)	EAFD (wt%)	LKW (wt%)	w/c ratio
REF	**100**	**-**	**-**	**1:0.29**
1EA-LK	98.94	1	0.06	1:0.29
2EA-LK	97.86	2	0.14	1:0.30
3EA-LK	96.80	3	0.2	1:0.30
5EA-LK	94.66	5	0.34	1:0.29
10EA-LK	89.32	10	0.68	1:0.30
1EA	99.00	1	-	1:0.29
2EA	98.00	2	-	1:0.30
3EA	97.00	3	-	1:0.30
5EA	95.00	5	-	1:0.29
10EA	90.00	10	-	1:0.30

Table 4 – **EAFD and LKW elementary chemical composition**

Element	EAFD (wt%)	LKW (wt%)
Fe	31.30	0.07
Zn	24.06	0.15
Ca	1.82	51.66
Cl	2.60	0.14
Na	1.21	0.89
Mn	1.71	0.00
Mg	1.17	0.27
K	0.99	0.03
Pb	0.98	0.0014
Cd	0.01	<0.0002
S	0.42	0.09
Al	0.38	0.13
Si	0.10	0.31
Cr	0.29	<0.0008
Cu	0.24	0.00
Sr	0.01	0.21
P	<0.00001	0.13
Ti	0.05	0.01
Ni	0.03	<0.0009
Sn	0.03	<0.001
Mo	0.01	<0.0003
Co	0.00	<0.0001
Moisture content at 105 °C (%)	1.63	2.85
Loss on ignition at 550 °C (%)	2.78	12.65
Loss on ignition at 950 °C (%)	4.21	13.81

Figure 2 – **Granulometric distribution of cement, EAFD and LKW**

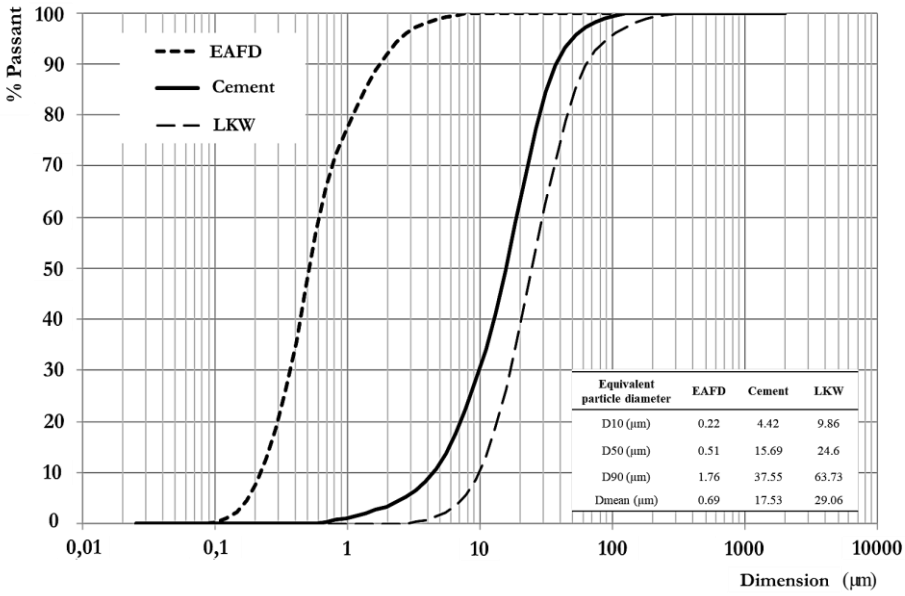

Note: D_{10}, D_{50}, D_{90} and D_{mean}: diameter of particles in 10%, 50%, 90% and mean of the retained fraction.

Table 5 shows the results for specific mass and surface area for cement, EAFD and LKW. EAFD had a higher specific mass (4.21 g/cm^3) while LKW had the smallest (2.37 g/cm^3). Measured specific mass for EAFD was similar to the result of 4.44 g/cm^3 obtained by Brehm *et al*. (2017). This suggested that adding EAFD increased the specific mass of the resulting cement while LKW had the opposite effect. EAFD presented a larger surface area (3.75 m²/g), followed by LKW (1.26 m²/g) and cement (1.20 m²/g). LKW,

despite having a larger surface area than cement, also had a larger particle size which was believed to be related to its porosity. Other studies noted that surface area affects cement reactivity and physio-mechanical properties such as rheology, hydration kinetics and resistance (MANTELLATO; PALACIOS; FLATT, 2015).

Micro-structural characterization of EAFD and LKW waste

Figures 3 and 4 and Tables 6 and 7 present the characterization of the main crystalline compounds in EFAD and LKW based on phases quantified by Rietveld refinement.

The EAFD diffractogram shown in Figure 3 shows a superposition of peaks between the desired phases. Rietveld refinement detected the presence of 9 crystalline phases, confirming the results of Brehm *et al.* (2017), Machado *et al.* (2006) and Bruckard *et al.* (2005). The phases detected were $ZnFe_2O_4$, Fe_3O_4, ZnO, $CaFe_2O_4$, $Mg(Fe_2O_4)$, SiO_2, KCl, MgO and Mn_3O_4, which are also shown in Table 6.

Tables 6 and 7 contain the R_w, R_{exp} and GOF Rietveld refinement factors. It is noted that according to Toby (2006), a condition of $R_w^2/R_{exp}^2 < 4$ indicated good refinement. Table 6 shows that EAFD contained mostly $ZnFe_2O_4$ (17.86 wt%), Fe_3O_4 (16.48 wt%) and ZnO (16.22 wt%) phases. This was not surprising since Fe and Zn are the predominant elements present in EAFD as seen in Table 4. One phase containing Ca ($CaFe_2O_4$) with 13.3 wt% can be identified from peak superposition in Figure 3. Brehm *et al.* (2017), Vargas, Masuero and Vilela (2006) and Machado *et al.*(2006) also identified phases containing Ca but in a different stoichiometric ratio ($Ca_{0,15}Fe_{2,82}O_4$). Magnesium was identified in phases $Mg(Fe_2O_4)$ and MgO with 12.26 wt% and 7.05 wt%, respectively. This was in agreement with Table 4, which showed 1.17 wt% of Mg in EAFD. Silicon dioxide, present in 7.82 wt%, was identified in 2θ positions in unique, superimposed peaks confirming the presence of Si in EAFD.

Table 5 – **Specific mass and specific surface area**

Paste	Especific mass (g/cm^3)	Specific surface area (m^2/g)
EAFD	4.21	3.75
Cement	3.06	1.20
LKW	2.37	1.26

Figure 3 – **Diffractogram with phase quantification by the Rietveld method of the EAFD sample**

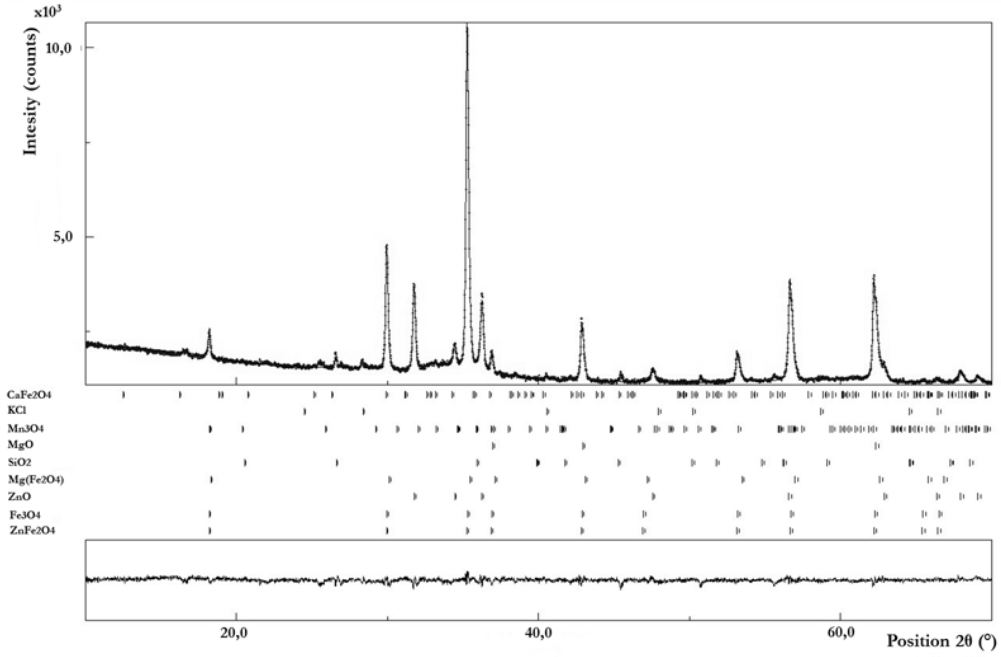

Table 6 – **Quantification of the phases present in the EAFD sample**

Phases	Crystallographic sheets	wt%
$ZnFe_2O_4$	ICSD: 75097	17.86
Fe_3O_4	COD: 1010369	16.48
ZnO	ICSD: 31052	16.22
$CaFe_2O_4$	ICSD: 158770	13.33
$Mg(Fe_2O_4)$	ICSD: 152467	12.26
SiO_2	COD: 5000035	7.84
KCl	ICSD: 165593	7.43
MgO	COD: 9000500	7.05
Mn_3O_4	ICSD: 30005	1.5
R_w= 2.81; R_{exp}= 2.52; GOF= 1.11		

Note: ICSD: Inorganic Crystal Structure Database; COD: Crystallography Open Database;R_w: weighted profile index; R_{exp}: expected profile index; and GOF: goodness-of-fit.

Figure 4 identifies five crystalline phases in LKW: $Ca(OH)_2$, $CaCO_3$, SiO_2, $Mg(CO)_33H_2O$ and $Ca_2Fe_2O_5$ which are further shown in Table 7. It can be seen in Table 7 that phases containing Ca in the form of $Ca(OH)_2$ (59.18 wt%) and $CaCO_3$ (18.97 wt%) are predonimant in LKW. This result was in agreement with Table 4 in which Ca represents 51.66 wt% of LKW and the losses on ignition at 550 ^oC and 950 ^oC corresponded to the dihydroxylation of $Ca(OH)_2$ and decomposition of $CaCO_3$, respectively. Surprisingly, Table 7 shows a lack of CaO in LKW. LKW is formed when the lime furnace operation is interrupted and $CaCO_3$ breaks down into CaO and CO_2 through the causticizing process. Consequently, some CaO was expected to remain in the sample. However, material used in this study was not collected immediately after being generated; rather LKW was kept exposed to the weather in an open-air storage area from which samples were taken at a later time. Under these conditions, CaO reacts with water and CO_2 to form $Ca(OH)_2$ and $CaCO_3$. Silicon dioxide accounted for 15.61 wt% and was identified in 2θ positions in isolated and superimposed peaks. The presence of SiO_2 in the LKW sample could also be attributed to exposure to elements caused by storage conditions.

Setting times and semi-adiabatic temperature results

Figure 5 displays the average initial and final setting time for each cement paste type and their corresponding final setting time deviation. Results allowed the determination of the effect of EAFD substitution in curbing initial setting time delay. Overall, there seemed to be an increase in setting time with increasing EAFD ratio (AL-ZAID; AL-SUGAIR; AL-NEGHEIMISH,1997; VARGAS; MASUERO; VILELA, 2006; FARES *et al.*, 2016; BREHM *et al*., 2017). The REF paste presented a final setting time of 3h 26min (marked as a red line in Figure 5) which was consistent with the reference value for CPV-ARI cement of 3h 14min, shown in Table 1. Paste 1EA-LK, with the lowest LKW substitution, resulted in a final setting time of 4h 02min – an increase of 17.5% with respect to the REF value. Paste 1EA-LK also presented the shortest setting time amongst all substitute cement pastes tested. In comparison, paste 1EA which did not contain LKW presented an increase in setting time of 1h 21m, which corresponded to a 39% increase with respect to the REF value.

Regarding initial setting time, Figure 5 shows a variation between the shortest time of 1h 33min (2EA) and the longest time of 5h 07min (5EA-LK). In general, the addition of EAFD resulted in a reduction in initial setting time when compared to REF. Although for paste 2EA, this reduction was excessive (over 1h shorter than REF). However, even if paste 2EA did not present the same trend as the others, the result was within the stipulated cement setting time (≥ 60 min) in NBR 16697 (ABNT, 2018c). Cement pastes with EAFD and LKW had initial setting times longer than REF and consequently also longer than any equivalent paste with EAFD substitution only. The increase in setting time caused by LKW substitution may be desirable when longer application times are needed.

Further addition of LKW had the opposite effect and caused an increase in setting time. The time increase could be related to the level of calcium zincate formed according to the quantity of LKW added. Paste 5EA remained within the required 10h to 12h technical time frame suitable for application of cement listed in NBR 16697 (ABNT, 2018c) even if the final setting time was 6h 43min longer than REF. Pastes 5EA-LK, 10EA and 10EA-LK had setting times of 17h 40min, 19h 46 min and 23h 06min, respectively, which exceeded the limit stipulated by NBR 16697 (ABNT, 2018c).

Figure 4 – **Diffractogram with quantification of phases by the Rietveld Method of the LKW sample**

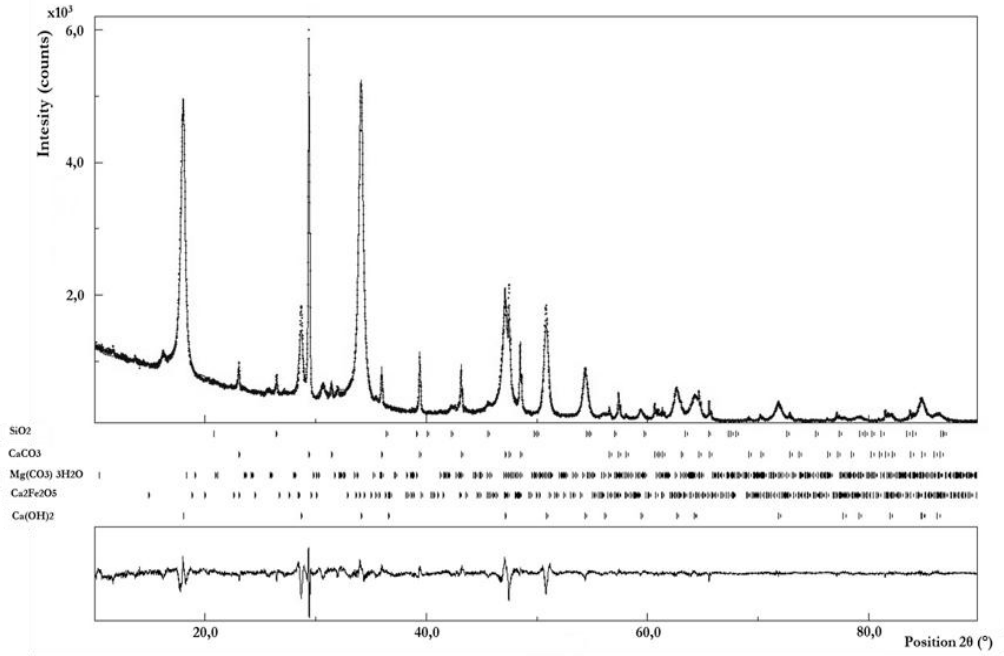

Table 7 – **Quantification of the phases present in the LKW sample**

Phases	Crystallographic sheets	wt%
$Ca(OH)_2$	ICSD: 15471	59.18
$CaCO_3$	ICSD: 18164	18.97
SiO_2	COD: 5000035	15.61
$Mg(CO)_3 3H_2O$	ICSD: 91710	5.27
$Ca_2Fe_2O_5$	ICSD: 14296	0.93
R_w: 8.09; R_{exp}: 4.19; GOF: 1.92		

Note: ICSD: Inorganic Crystal Structure Database; COD: Crystallography Open Database;R_w: weighted profile index; R_{exp}: expected profile index; and GOF: goodness-of-fit.

Figure 5 – **Results of cement pastes: initial, final setting time and final setting time of REF paste (red line)**

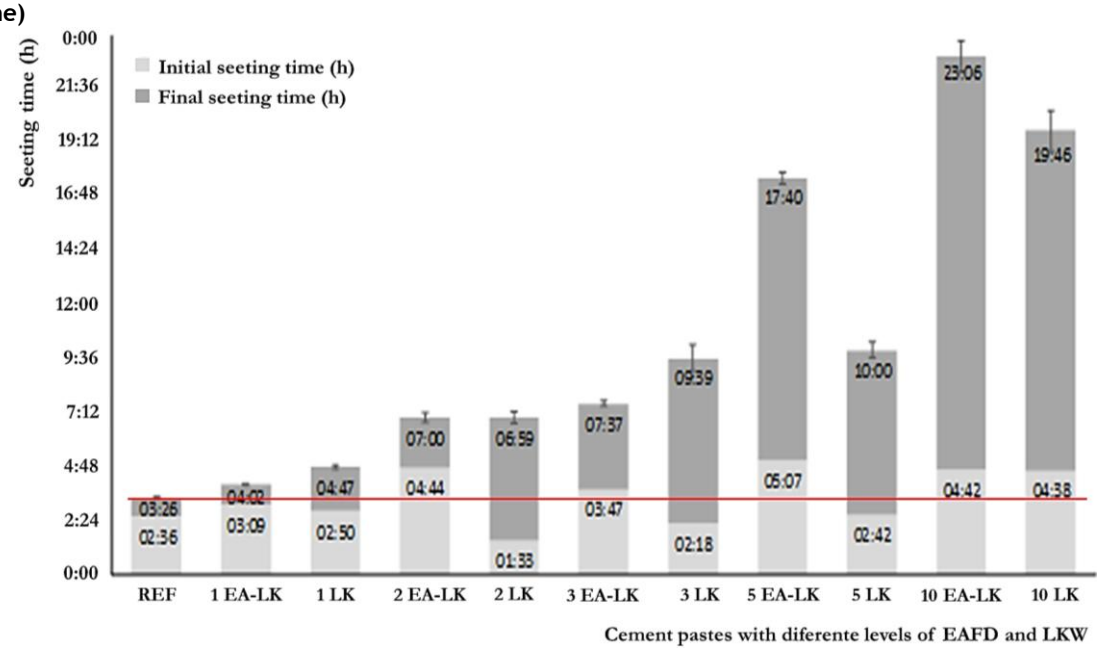

Overall, measured setting times were similar to results obtained from other references even though the Zn content of 24.06 wt% in EAFD was higher than others studies conducted in Brazil (ARNOLD; VARGAS, 2015; MACHADO *et al.*, 2006; SILVA, 2006; BREHM *et al.*, 2001; DUTRA; PAIVA; TAVARES, 2006; MARQUES SOBRINHO, 2012; MARTINS; REIS NETO; CUNHA, 2008).

Figure 6 shows semi-adiabatic temperature time-evolution of the cement pastes. Higher EAFD substitution had the direct effect of shifting temperature curves towards longer time periods. Comparison of the pastes with EAFD + LKW (EA-LK) and those without LKW (EA) showed that there was no uniform shift in the time curves with this regard. For example, a noticeable shift was present between samples 3EA-LK and 3EA with the temperature rise or acceleration of the 3EA sample starting earlier than 3EA-LK but the shape of the curves and peak temperatures remained similar.

According to Mehta and Monteiro (2014), setting time develops in the temperature rise or acceleration period. Pastes 10EA-LK and 10EA had the largest time shift compared to the other pastes. Paste 10EA presented earlier temperature acceleration than paste 10EA-LK and clearly attained a higher peak temperature. Overall, pastes without LKW (EA) had earlier temperature acceleration, indicating that the addition of LKW and EAFD at these levels delayed initial setting time. Effect on acceleration periods itself varied: pastes REF, 1EA-LK, 1EA, 2EA-LK and 2EA had similar acceleration periods of 4h but once EAFD substitution reached 3 wt% and higher, acceleration time increased to 5h 37min (5EA-LK) and 8h 20min (10EA). Peak temperature remained close to 100 ºC for pastes REF, 1EA-LK, 1EA, 2EA-LK and 2EA but once EAFD substitution reached 3 wt% and higher, peak temperatures dropped considerably with the lowest peak of 51.9 ºC for paste 10EA-LK.

Figure 7 shows more closely the semi-adiabatic temperature time-evolution of pastes REF, 1EA-LK and 1EA. Peak temperatures for the pastes were achieved in 9h, 8h 50min and 8h 40min, respectively. Temperature evolution curves between pastes 1EA-LK and 1EA were similar to REF with regards to acceleration and deceleration times. These trends agreed with results from Vargas, Masuero and Vilela (2006) which studied hydration heat in semi-adiabatic recipients for Portland cement II-Z 32 with 0, 5, 15 and 25 wt% EFAD substitution. They also reported the time increase effect and peak temperature decrease with increasing levels of EAFD. For their study, the peak acceleration times were observed at 10h (0 wt%), 22h (5 wt%), 46h (15 wt%) e 78h (25 wt%).

Figure 6 - **Time-evolution of semi-adiabatic temperature results on cement pastes**

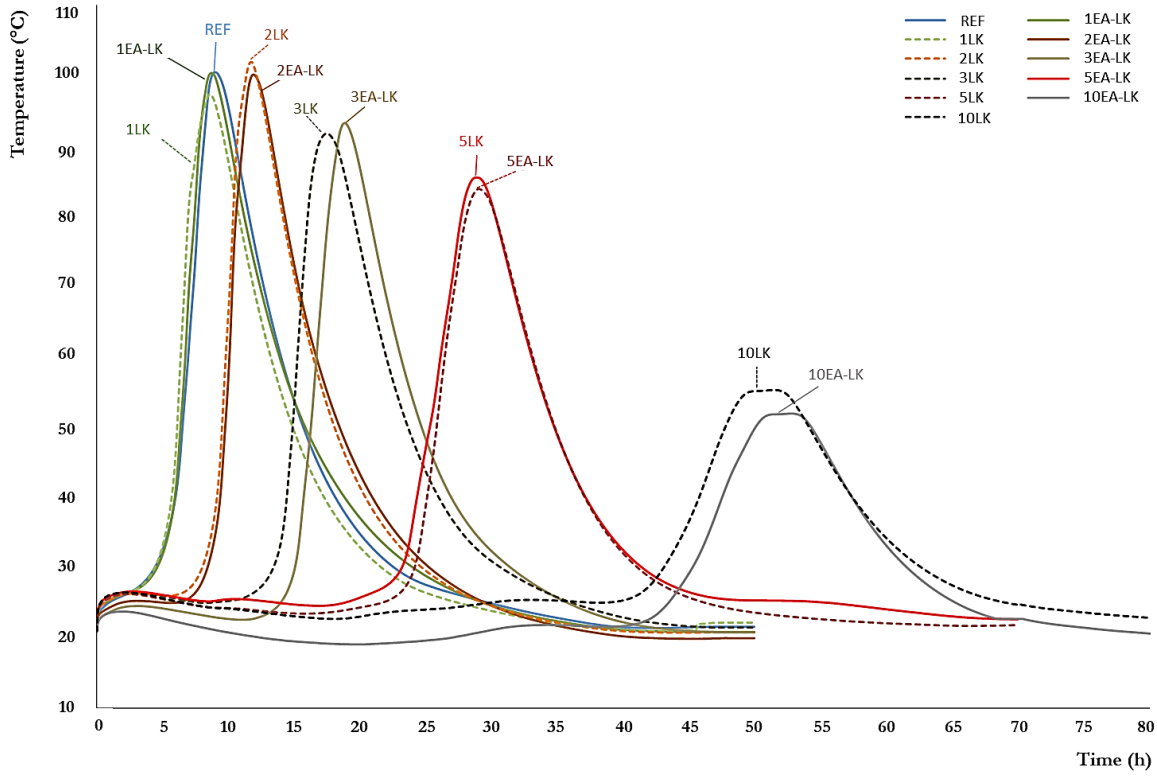

Figure 7 – **Evolution of semi-adiabatic temperature for REF, 1EA-LK and 1EA cement pastes**

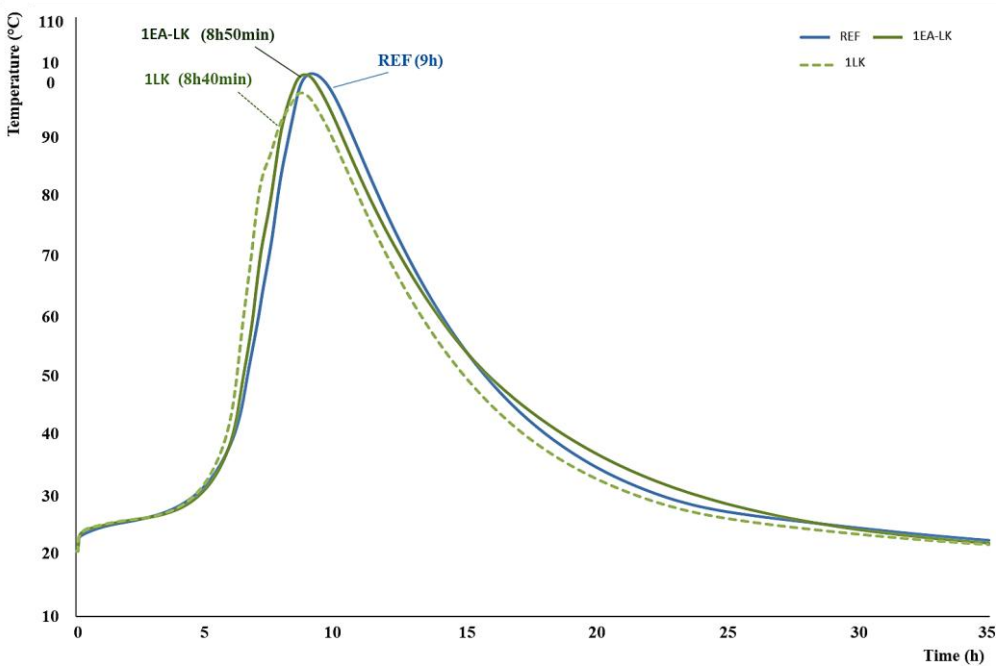

Figures 6 and 7 demonstrate that semi-adiabatic temperature evolution times were longer than setting times. Final setting time for REF was 3h 26min while the temperature-based corresponding hardening time was longer than 9h. For paste 10EA-LK, final setting time was measured as 23h 06min but the temperature-based hardening time was of around 50h. Vargas, Masuero and Vilela (2006) observed similar time differences in tests conducted under ABNT guidelines to measure setting time and hydration enthalpy to obtain the temperature time-evolution of the hydration process. Similar results were also reported by Fares *et al*. (2016) with an automated Vicat apparatus for the same properties measured by Vargas, Masuero and Vilela (2006). Vargas (2002) did not obtain coherent setting time results for EAFD substitution using a Vicat apparatus and opted instead to use hydration heat tests to determine setting times. Results from Vargas (2002) were not in agreement with trends observed in this study, which measured paste 2EA with a shorter setting time than REF and paste 5EA-LK with a longer setting time than paste 5EA. The variation between studies could be attributed to the testing procedures defined in NBR 16607 (ABNT, 2018b) which gives rise to uncertainties depending to the technique chosen to measure setting time. For this reason, this study also measured semi-adiabatic temperature evolution as a comparison tool.

Phase detection by X-ray Diffraction (XRD) and Rietveld refinement

The phases detected in the pastes were identified by X-ray Diffraction (XRD) and complemented with Rietveld refinement. Table 8 shows the phases detected for pastes REF, EA and EA-LK aged 1 day, 4 days and 7 days. Results were presented through a detection scale: "nd" for no detection, "*" for less than 5 wt%, "**" for between 5 wt% - 30 wt% and "***" for more than 30 wt%. This was chosen because percentages measured in this study presented variations different than reference works, which suggested the need to improve data acquisition and analysis techniques. Thus, the chosen scale was selected in order to better visualize trends and relate the present results to the ones obtained in other studies. Besides the common phases identified for anhydrous and hydrated cement, the pastes of this study had common compounds present in EAFD such as $ZnFe_2O_4$, ZnO e Fe_3O_4. Paste REF presented the same phases after 1 day and 4 days but $CaCO_3$ was no longer detected after 7 days. The characteristic peaks of each phase were superimposed except for phases $Ca(OH)_2$ at position 17.89° 2θ and $CaCO_3$ at position 29.41° 2θ. Phases characteristic of hydrated and anhydrous cement (Ca_3SiO_5, $Ca(OH)_2$, $Ca_2(SiO_3)(OH)_2$ and $Ca_6Al_2(OH)_{12}(SO_4)_326H_2O$) were identified in paste REF for all 3 ages tested. Phases with mass exceeding 30 wt% were $Ca(OH)_2$ (aged 1 day, 4 day and 7 days) and Ca_3SiO_5 (aged 7 days) but phases $CaSO_42H_2O$ and Ca_2SiO_4 present in anhydrous cement were not detected. Phases detected in quantities under 5 wt% were CaO, Al_2O_33CaO, $Ca_2(SiO_3)$ $(OH)_2$, $Ca_6Al_2(OH)_{12}(SO_4)_326H_2O$ and SiO_2 (aged 1 day, 4 days and 7 days),

$Ca_2(FeAl)O_5$ and Ca_3Si2O_7 (aged 4 days and 7 days), MgO (aged 1day and 7 days) and $CaCO_3$ (aged 4 days). Detection of $CaCO_3$ could be attributed to carbonate filler added to Portland cement CPV – ARI which, under NBR 16697(ABNT, 2018c), can contain up to 10% of mineral additives. In EA pastes, a reduction in the number of phases was observed with hydration. Phases $CaSO_40$, $5H_2O$, SiO_2, Al_2SiO_5 and $K_2Mg_2(SO_4)_3$ were not detected after 4 days and phases $Ca_6Al_2(OH)_{12}(SO_4)_326H_2O$ and $CaSO_42H_2O$ were not detected after 7 days. On the other hand, EA-LK pastes had an increase in the number of phases with hydration. Phases $CaCO_3$, ZnO and $Ca_6Al_2(OH)_{12}(SO_4)_326H_2O$ were detected after 4 days and 7 days. In particular, $Ca_6Al_2(OH)_{12}(SO_4)_326H_2O$ formed at the initial stages of hydration and was a characteristic of the acceleration period (MEHTA; MONTEIRO, 2014; QUARCIONI, 2008; BULLARD *et al*., 2011; RIDI *et al*., 2011; HU; GE; WANG, 2014). The lack of this compound after 1 day suggested a lack of hydration effect which was in agreement with the similarity of semi-adiabatic temperature curves between REF, 1EA and 1EA-LK. However, for paste 1EA, $Ca_6Al_2(OH)_{12}(SO_4)_326H_2O$ was detected after 1 day and 4 days but not after 7 days. Since the amount of LKW added was low (around 0,06 wt%), this was unlikely to be associated with waste addition.

With regards to compounds present from EAFD substitution, Table 8 shows that phases for $ZnFe_2O_4$ were less than 5 wt% for paste 1EA-LK after 1 day and 7 days and less than 5 wt% for 1EA after 1 day, 4 days and 7 days. Quantities of ZnO were also detected at less than 5 wt% after 4 days and 7 days. In contrast, Fe_3O_4 with quantities between 5 wt% and 30 wt% was detected only for paste 1EA-LK at 4 days. Also, no calcium zincate ($CaZn_2(OH)_62H_2O$) was detected in both EA-LK and EA pastes which had less than 1 wt% of EAFD substitution. The ICP analysis of Table 4 shows a 24.06 wt% of Zn in EAFD so the resulting Zn content in cement was approximately 0.24 wt%. Mellado *et al.* (2013) evaluated the effect of 0.1 wt% of Zn in a C_3S sample with 28 days of curing time. Results showed that the cement paste presented traces of $CaZn_2(OH)_6.2H_2O$ e $Ca(OH)_2$ with low-intensity peaks. In comparison, the present study, with 1 wt% of Zn and the same curing time, detected no $Ca(OH)_2$ and only traces of $CaZn_2(OH)_6.2H_2$. Consequently, the lack of calcium zincate in pastes 1EA-LK and 1EA could be related to their self-similarity of semi-adiabatic temperature time-evolution and their similarity to REF.

Table 8 - **Detected phases in cement pastes by the Rietveld Method**

Phases	Crystallographic sheets	REF			1EA-LK			1EA			10EA-LK		10EA	
		1 day	4 days	7 days	1 day	4 days	7 days	1 day	4 days	7 days	4 days	7 days	4 days	7 days
$Ca(OH)_2$	ICSD: 15471	***	***	***	**	**	***	***	***	***	**	**	**	**
$CaCO_3$	ICSD: 18164	**	*	nd	Nd	*	*	*	**	*	*	*	*	*
CaO	ICSD: 51409	*	*	*	Nd	nd	nd	Nd	nd	nd	nd	nd	nd	nd
Ca_2SiO_4	COD: 9012792	nd	nd	nd	*	**	*	**	*	**	**	**	**	**
Ca_3SiO_5	COD: 9015421	**	**	***	***	**	***	***	***	**	***	**	***	*
$Ca_3Si_2O_7$	COD: 9012094	**	*	*	nd	nd	nd	Nd	nd	nd	nd	nd	nd	nd
Al_2O_3 3CaO	ICSD: 151369	*	*	*	nd	nd	nd	Nd	nd	nd	nd	nd	nd	nd
$Ca_2(SiO_3)(OH)_2$	ICSD: 80127	*	*	*	*	*	*	nd	*	**	*	**	*	***
$CaZn_2(OH)_62H_2O$	ICSD: 50178	nd	nd	nd	nd	nd	nd	nd	nd	nd	*	*	**	**
$ZnFe_2O_4$	ICSD: 75097	nd	nd	nd	*	nd	*	*	*	*	*	*	**	**
ZnO	ICSD: 31052	nd	nd	nd	nd	*	*	nd	nd	nd	*	**	*	*
Fe_3O_4	COD: 1010369	nd	nd	nd	nd	**	nd	nd	nd	nd	*	**	*	*
$Ca_2Fe_2O_5$	ICSD: 14296	nd	nd	nd	nd	nd	nd	nd	nd	nd	*	*	*	*
$Ca_2(FeAl)O_5$	ICSD: 9197	**	*	*	**	*	**	**	**	**	nd	nd	nd	nd
$Ca_6Al_2(OH)_{12}(SO_4)_326H_2O$	ICSD: 155395	*	*	*	nd	*	*	*	*	nd	*	nd	*	*
$CaSO_42H_2O$	ICSD: 2058	nd	nd	nd	*	nd	*	*	*	nd	nd	nd	nd	nd
$CaSO_40,5H_2O$	ICSD: 69060	nd	nd	nd	nd	nd	nd	*	nd	nd	nd	nd	nd	nd
MgO	COD: 9000500	*	**	*	*	**	**	*	**	*	*	**	*	**
SiO_2	COD: 5000035	*	*	*	*	nd	*	*	nd	nd	*	*	*	*
$CaAl_2O_4$	ICSD: 157457	nd	nd	nd	nd	nd	nd	nd	*	*	nd	nd	nd	nd
Al_2SiO_5	ICSD: 30679	nd	nd	nd	nd	nd	nd	*	nd	nd	nd	nd	nd	nd
K_2SO_4	ICSD: 2408	nd	nd	nd	*	*	*	*	*	*	nd	nd	nd	nd
$K_2Mg_2(SO_4)_3$	ICSD: 100420	nd	nd	nd	*	nd	*	*	nd	*	nd	nd	nd	nd
$CaMgSi_2O_6$	ICSD: 5205	nd	nd	nd	nd	nd	nd	nd	nd	nd	*	*	**	*
R_w		5.54	5.91	4.7	4.36	6.37	4.6	5.54	5.59	4.82	5.32	4.55	4.02	5.89
R_{exp}		3.93	3.84	3.87	3.63	3.75	3.74	3.91	3.77	3.93	3.48	3.69	3.73	3.61
GOF		1.4	1.53	1.21	1.2	1.69	1.23	1.41	1.48	1.22	1.52	1.23	1.07	1.63

Note: * = mass < 5 wt%; ** = mass between 5 wt% and 30 wt%; *** = mass >30 wt%; nd: not detected; "ICSD = Inorganic Crystal Structure Database; COD = Crystallography Open Database; R_w: = weighted profile index; R_{exp}: = expected profile index; and GOF = goodness-of-fit."

According to Mellado *et al.* (2013) and Weeks, Hand and Sharp (2008), $Ca(OH)_2$ is formed late, towards the end of the initial ages in pastes containing Zn due to calcium zincate generation. Calcium hydroxide was detected with over 30 wt% in pastes 1EA-LK after 7 days and 1EA at all ages, which was similar to REF. With regards to $Ca_2(SiO_3)(OH)_2$ REF and paste 1EA-LK detected less than 5 wt% at all ages but paste 1EA had no detection after 1 day, less than 5 wt% after 4 days and between 5 wt% to 30 wt% after 7 days. EAFD substitution in 1EA-LK and 1EA pastes reduced the quantity of hydration compounds ($Ca(OH)_2$, $Ca_2(SiO_3)(OH)_2$ e$Ca_6Al_2(OH)_{12}(SO_4)_326H_2O$) but with no significant effect on semi-adiabatic temperature when compared to REF.

For pastes 10EA-LK and 10EA, the low number of peaks after 1 day did not allow for Rietveld refinement. However paste 10EA-LK after 4 days and paste 10EA after 4 days and 7 days presented 14 phases: $Ca(OH)_2$, $CaCO_3$, Ca_2SiO_4, $Ca_6Al_2(OH)_{12}(SO_4)_326H_2O$, Ca_3SiO_5, $Ca_2(SiO_3)(OH)_2$, $CaZn_2(OH)_62H_2O$, $ZnFe_2O_4$, ZnO, Fe_3O_4, $Ca_2Fe_2O_5$, MgO, SiO_2 and $CaMgSi_2O_6$. This suggested that after only 1 day, many peaks were superimposed so that clear phase identification was not possible. The phases detected due to EAFD substitution in pastes 10EA-LK and 10EA were the same as pastes 1EA-LK and 1EA but in larger quantities. This was not surprising since EAFD content in pastes 10EA-LK and 10EA was 10 wt%. Phase $ZnFe_2O_4$ was detected with less than 5 wt% in paste 10EA-LK and between 5 wt% and 30 wt% for paste 10EA. Phases ZnO and Fe_3O_4 were detected with less than 5 wt% in paste 10EA-LK after 4 days and between 5 wt% and 30 wt% after 7 days while paste 10EA remained at less than 5 wt% after 4 days and 7 days. Vargas, Masuero and Vilela (2006) also detected $ZnFe_2O_4$ and Fe_3O_4 in cement pastes with 5 wt%, 15 wt% and 25 wt% of EAFD (13.3 wt% of Zn) at 7 days and 28 days but did not detect ZnO. Consequently, the presence of ZnO in this study could also be attributed to the Zn content of the EAFD used, which was much higher (24.06 wt%). With regards to calcium zincate ($CaZn_2(OH)_62H_2O$), pastes 10EA-LK and 10EA had different results: less than 5 wt% for paste 10EA-LK and between 5 wt% and 30 wt% for paste 10EA after the same 4 days and 7 days. Calcium zincate presence is associated with the Zn content in cement, as reported by Brehm *et al.* (2017), Vargas, Masuero and Vilela (2006) and Mellado *et al.* (2013). The presence of calcium zincate in pastes 10EA-LK and 10EA and its lack-off in pastes 1EA-LK and 1EA could be considered as one of the factors that resulted in different semi-adiabatic temperature curves of Figure 5. As in REF and pastes 1EA-LK and 1EA, phase $Ca(OH)_2$ was also detected in pastes 10EA-LK and 10EA but in smaller amounts. According to Mellado *et al.* (2013), cement pastes with high levels of EAFD substitution had more phases containing Zn and lower quantities of $Ca(OH)_2$, which suggested an inhibiting effect of Zn in $Ca(OH)_2$ formation and cement hydration. Phase $Ca_2(SiO_3)(OH)_2$ was also detected in pastes 10EA-LK and 10EA in quantities superior to other pastes. This is contradictory in the sense that, due to the high level of EAFD substitution and its effect in delaying initial setting time, less $Ca_2(SiO_3)(OH)_2$ was expected. Contrary to this, over 30 wt% was detected in paste 10EA after 7 days along with elevated diffraction peak superposition, which points to a possible sampling issue.

Conclusions

(a) results from EAFD phase detection by XRD indicated a polycrystalline waste predominantly with $ZnFe_2O_4$, ZnO, Fe_3O_4 and $CaFe_2O_4$. In contrast, LKW characterization showed polycrystalline waste with predominant $Ca(OH)_2$ and $CaCO_3$ phases;

(b) there was a direct relation between increasing levels of EAFD substitution and increasing final setting time for cement pastes. Pastes samples with the least amount of EAFD subsitution (1EA-LK, 1EA, 2EA-LK, 2EA, 3EA-LK, 3EA and 5EA-LK) had the least change in setting time according to what is stipulated for cement by NBR 16697 (ABNT, 2018c);

(c) pastes 1EA-LK e 1EA contained phases common to EAFD ($ZnFe_2O_4$, ZnO and Fe_3O_4) as well as those from cement hydration ($Ca(OH)_2$, $Ca_2(SiO_3)(OH)_2$ and $Ca_6Al_2(OH)_{12}(SO_4)_326H_2O$);

(d) calcium zincate ($CaZn_2(OH)_62H_2O$) was not identified in pastes 1EA-LK and 1EA and was only present in pastes 10EA-LK and 10 EA. This indicated that part of calcium ion (Ca^{2+}) was being formed in this phase;

(e) semi-adiabatic temperature evolution confirmed the trend of increase in setting time delay with increasing waste substitution. Pastes 1EA-LK and 1EA presented evolution curves similar to REF;

(f) peak temperature reductions were observed in semi-adiabatic temperature evolutions for EAFD substitution of 3 wt% and higher (paste 3EA). This result suggested that EAFD could be used in situations in which reductions in cement hydration heat are desired, such as large foundation blocks or dams; and

(g) pastes 1EA (EAFD substitution) and 1EA-LK (EAFD+LKW substitution) presented a hydration heat similar to REF. This suggested that for the level of substitution of these cases, EAFD+LKW did not affect significantly the hydration reactions in cement and their use in construction materials would be a viable waste recycling technique.

References

AIQIN, W.; CHENGZHI, Z.; NINGSHENG, Z. The theoretic analysis of the influence of the particle size distribution of cement system on the property of cement. **Cement and Concrete Research**. v. 29, p. 1721-1726, 1999.

AL-ZAID, R. Z.; AL-SUGAIR, F. H.; AL-NEGHEIMISH, A. I. Investigation of potential uses of electric-arc furnace dust (EAFD) in concrete. **Cement and Concrete Research**, v. 27, n. 2, p. 267-278, 1997.

ALARCON-RUIZ, L. *et al.* The use of thermal analysis in assessing the effect of temperature on a cement paste. **Cement and Concrete Research**, v. 35, p. 609–613, 2005.

ARNOLD, M. C.; VARGAS, A. S; BIANCHINI, L. Study of electric-arc furnace dust (EAFD) in fly ash and rice husk ash-based geopolymers. **Advanced Powder Technology,** v. 28. p. 2023–2034, 2017.

ARNOLD, M. C.; VARGAS, A. S. Estudo da viabilidade técnica do uso do pó de aciaria elétrica em geopolímeros. In: CONGRESSO ANUAL DA ABM - INTERNACIONAL, 70., Rio de Janeiro, 2015. **Anais [...]** São Paulo: Associação Brasileira de Metalurgia, Materiais e Mineração, 2015.

ASSOCIAÇÃO BRASILEIRA DE FUNDIÇÃO. **CEMP (Comissão de Estudos de Matérias Primas) n° 120: Materiais para Fundição**: determinação da perda ao fogo. São Paulo: ABIFA, 2003.

ASSOCIAÇÃO BRASILEIRA DE NORMAS TÉCNICAS. **NBR 10007**: amostragem de resíduos sólidos. Rio de Janeiro, 2004.

ASSOCIAÇÃO BRASILEIRA DE NORMAS TÉCNICAS. **NBR 16606**: cimento Portland: determinação da pasta de consistência normal. Rio de Janeiro, 2018a.

ASSOCIAÇÃO BRASILEIRA DE NORMAS TÉCNICAS. **NBR 16607**: cimento Portland: determinação do tempo de pega. Rio de Janeiro, 2018b.

ASSOCIAÇÃO BRASILEIRA DE NORMAS TÉCNICAS. **NBR 16697**: cimento Portland: requisitos.Rio de Janeiro, 2018c.

BREHM, F. A. *et al.* Caracterização química, térmica e estrutural de pós de aciaria elétrica. In: SEMINÁRIO DE FUSÃO, REFINO E SOLIDIFICAÇÃO DOS METAIS, 32., Salvador, 2001. **Anais [...]** Salvador, 2001.

BREHM, F. A. *et al.* Oxide zinc addition in cement paste aiming electric arc furnace dust (EAFD) recycling. **Construction and Building Materials**, v. 139, p. 172–182, 2017.

BRUCKARD, W. J. *et al.* Water leaching and magnetic separation for decreasing the chloride level and upgrading the zinc content of EAF steelmaking baghouse dusts. **International Journal of Mineral Processing,** v. 75, p. 1–20, 2005.

BULLARD, J. W. *et al.* Mechanisms of cement hydration. **Cement and Concrete Research**, v. 41, p. 1208-1233, 2011.

BURUBERRI, L. H.; SEABRA, M. P.; LABRINCHA, J. A. Preparation of clinker from paper pulp industry wastes. **Journal of Hazardous Materials**, v. 286, p. 252–260, 2015.

CARRANZA, F. *et al.* Recovery of Zn from acid mine water and electric arc furnace dust in an integrated process. **Journal of Environmental Management**, v. 165, p. 1715-183, 2016.

COMPANHIA DE CIMENTO ITAMBÉ. **Relatórios de ensaio.** 2015. Available: http://www.cimentoitambe.com.br. Access in: 07 December 2015.

CUBUKCUOGLU, B.; OUKI, S. K. Solidification/stabilization of electric arc furnace waste using low grade MgO. **Chemosphere**, v. 86, p. 789–796, 2012.

DUTRA, A. J. B.; PAIVA, P. R. P.; TAVARES, L. M. Alkaline leaching of zinc from electric arc furnace steel dust. **Minerals Engineering**, v. 19, p. 478–485, 2006.

FARES, G. *et al.* Performance of optimized electric arc furnace dust-based cementitious matrix compared to conventional supplementary cementitious materials. **Construction and Building Materials**, v. 112, p. 210–221, 2016.

FISCHER, C.; LEHENER, M.; MCKINNON, D.L. **Overview of the use of landfill taxes in Europe**. Available: https://ec.europa.eu/environment/waste/pdf/strategy/3.%20%20Christian%20Fischer%20EEA%20Landfill%20taxes.pdf. Access in: 07 Feb. 2019.

HU, J.; GE, Z.; WANG, K. Influence of cement fineness and water-to-cement ratio on mortar early-age heat of hydration and set times. **Construction and Building Materials**, v. 50, p. 657-663, 2014.

INDÚSTRIA BRASILEIRA DE ÁRVORES. **Relatório 2019**. Available in: https://www.iba.org/datafiles/publicacoes/relatorios/iba-relatorioanual2019.pdf. Access in: 29 Nov. 201.

INSTITUTO AÇO BRASIL. **Relatório de sustentabilidade 2018**: dados 2016/2017. Rio de Janeiro, 2018. Available in: http://www.acobrasil.org.br/sustentabilidade/. Access in: 29 Jul. 2019.

KAVOURAS, P. *et al.* Glass-ceramic materials from electric arc furnace dust. **Journal of Hazardous Materials**, v. A139, p. 424–429, 2007.

KNOP, Y.; PELED, A. Setting behavior of blended cement with limestone: influence of particle size and content. **Materials and Structures**, v. 49, p. 439-452, 2016.

MACHADO, J. G. M. S. *et al.* Chemical, physical, structural and morphological characterization of the electric arc furnace dust. **Journal of Hazardous Materials**, v. B136, p. 953-960, 2006.

MANTELLATO, S.; PALACIOS, M.; FLATT, R. J. Reliable specific surface area measurements on anhydrous cements.**Cement and Concrete Research**, v. 67, p. 286-291, 2015.

MARQUES SOBRINHO, V. P. F. **Adição de poeira de aciaria elétrica em ferro gusa líquido**. São Paulo, 2012. Doctoral Thesis – Programa de Pós-Graduação em Engenharia Metalúrgica e de Materiais, Universidade de São Paulo, São Paulo, 2012.

MARTINS, F. M.; REIS NETO, J. M.; CUNHA, C. J. Mineral phases of weathered and recent electric arc furnace dust. **Journal of Hazardous Materials**, v. 154, p. 417–425, 2008.

MASLEHUDDIN, M. *et al.* Effect of electric arc furnace dust on the properties of OPC and blended cement concretes. **Construction and Building Materials**, v. 25, p. 308–312, 2011.

MASSARWEH, O. *et al.* Development of a concrete set retarder utilizing electric arc furnace dust. **Construction and Building Materials**, v. 255, p. 1-11,2020.

MEHTA, P. K.; MONTEIRO, P. J. M. **Concreto**: microestrutura, propriedades e materiais. São Paulo: IBRACON, 2014.

MELLADO, A. *et al.* Inmobilization of Zn (II) in Portland cement paste: determination of microstructure and leaching performance. **Journal of Thermal Analysis and Calorimetry**, v. 112, n. 3, p. 1377-1389, 2013.

MENAD, N. *et al.* Study of the presence of fluorine in the recycled fractions during carbothermal treatment of EAF dust. **Waste Management**, v. 23, p. 483–491, 2003.

MODOLO, R. *et al.* Lime mud from cellulose industry as raw material in cement mortars. **Materiales de Construcción**, v. 64, n. 316, 2014.

MODOLO, R. *et al.* Pulp and paper plant wastes valorization in bituminous mixes. **Waste Management**, v. 30, p. 685–696, 2010.

NIUBÓ, M. *et al.* A possible recycling method for high grade steels EAFD in polymer composites. **Journal of Hazardous Materials**, v. 171, p. 1139–1144, 2009.

QUARCIONI, V. A. **Influência da Cal Hidratada nas Idades Iniciais da Hidratação do Cimento Portland**: estudo em pasta. São Paulo, 2008. Doctorate Thesis – Programa de Pós-graduação em Engenharia Civil, Escola Politécnica da Universidade de São Paulo, São Paulo, 2008.

RIDI, F. *et al.* Hydration kinetics of tricalcium silicate by calorimetric methods. **Journal of Colloid and Interface Science,** v. 364, p. 118–124, 2011.

SILVA, M. C. **Reciclagem de pó de aciaria elétrica como matéria-prima na fabricação de materiais cerâmicos argilosos**: controle das emissões atmosféricas de zinco.Porto Alegre, 2006. Doctorate Thesis – Programa de Pós-Graduação em Engenharia de Minas, Metalúrgica e de Materiais, Universidade Federal do Rio Grande do SUL, Porto Alegre, 2006.

SIQUEIRA, F. B.; HOLANDA, J. N. F. Reuse of grits waste for the production of soil-cement bricks. **Journal of Environmental Management**, v. 131, p. 1-6, 2013.

STEGEMANN, J. A. *et al.* Understanding environmental leachability of electric arc furnace dust. **Journal of Environmental Engineering**, v. 126, p. 112-120, 2000.

TOBY, B. H. R factors in Rietveld analysis: how good is good enough? **Powder Diffraction**, v. 21, n. 1, p. 67-70, 2006.

VARGAS, A. S. **Estudo da viabilidade do uso de PAE a arco na confecção de blocos de concreto para pavimentação.** Porto Alegre, 2002. Doctoral Thesis – Programa de Pós-Graduação em Engenharia de Minas, Metalúrgica e de Materiais, Universidade Federal do Rio Grande do SUL, Porto Alegre, 2002.

VARGAS, A. S.; MASUERO, A. B.; VILELA, A. C. F. Estudo microestrural e determinação de calor de hidratação em pastas de cimento Portland com pó de aciaria elétrica (PAE). **Ambiente Construído**, Porto Alegre, v. 4, n. 2, p. 7-18, abr./jun. 2004.

VARGAS, A. S.; MASUERO, A. B.; VILELA, A. C. F. Investigations on the use of electric-arc furnace dust (EAFD) in Pozzolan-modified Portland cement I (MP) pastes. **Cement and Concrete Research**, v. 36, p. 1833-1841, 2006.

WEEKS, C.; HAND, R. J.; SHARP, J. H. Retardation of cement hydration caused by heavy metals present in ISF slag used as aggregate. **Cement & Concrete Composites**, v. 30, p. 970–978, 2008.

WOLFF, E. **O uso do lodo de estação de tratamento de água e resíduos da indústria de celulose (*dregs, grits* e lama de cal) na produção de cerâmica vermelha**.Belo Horizonte, 2008. Doctoral Thesis – Programa de Pós-Graduação em Saneamento, Meio Ambiente e Recursos Hídricos, Universidade Federal de Minas Gerais, Belo Horizonte, 2008.

Acknowledgements

The authors thank Conselho Nacional de Desenvolvimento Científico e Tecnológico (CNPq) for the Technological Development Productivity Scholarship and Innovative Extension (authors Feliciane de Andrade Brehm and Carlos Alberto Mendes Moraes), Research Productivity Scholarship - Level 2 (author Regina Célia Espinosa Modolo). Phd Scholarship CAPES (author Marilise Garbin).

Josué Claudio Metz
Programa de Pós-Graduação em Engenharia Civil, Núcleo de Caracterização de Materiais | Universidade do Vale do Rio dos Sinos São Leopoldo – RS – Brasil | CEP 93022-750 | Tel.: (51) 3591-1122 | E-mail: josue.metz@gmail.com

Elenize Ferreira Maciel
Programa de Pós-Graduação em Engenharia Civil: Construção e Infraestrutura | Universidade Federal do Rio Grande do Sul | Av. Osvaldo Aranha, 99 | CEP 90035-190| Tel.: (51) 3308-4948 | E-mail: elenizefm@gmail.com

Marilise Garbin
Programa de Pós-Graduação em Engenharia Civil, Núcleo de Caracterização de Materiais | Universidade do Vale do Rio dos Sinos | E-mail: mgarbin@edu.unisinos.br

Regina Célia Espinosa Modolo
Programa de Pós-Graduação em Engenharia Civil e Mecânica, Núcleo de Caracterização de Materiais | Universidade do Vale do Rio dos Sinos | E-mail: reginaem@unisinos.br

Carlos Alberto Mendes Moraes
Programa de Pós-Graduação em Engenharia Civil e Mecânica, Núcleo de Caracterização de Materiais | Universidade do Vale do Rio dos Sinos | E-mail: cmoraes@unisinos.br

Lucas Bonan Gomes
Laboratório de Difratometria de Raios X | Universidade Federal do Rio Grande do Sul | Av. Bento Gonçalves, 9500, Prédio 43126, Sala 211 | Porto Alegre – RS – Brasil | Caixa Postal 15001 | CEP 91501-970 E-mail: lucas.gomes@ufrgs.br

Feliciane Andrade Brehm
Programa de Pós-Graduação em Engenharia Civil, Núcleo de Caracterização de Materiais | Universidade do Vale do Rio dos Sinos | E-mail: felicianeb@unisinos.br

Ambiente Construído
Revista da Associação Nacional de Tecnologia do Ambiente Construído
Av. Osvaldo Aranha, 99 - 3º andar, Centro
Porto Alegre – RS - Brasil
CEP 90035-190
Telefone: +55 (51) 3308-4084
Fax: +55 (51) 3308-4054
www.seer.ufrgs.br/ambienteconstruido
E-mail: ambienteconstruido@ufrgs.br